Hypoplastic model for crushable sand

Phuong, N. T.V.; Rohe, A.; Brinkgreve, R. B.J.; van Tol, A. F.

DOI
10.1016/j.sandf.2018.02.022

Publication date
2018

Document Version
Final published version

Published in
Soils and Foundations

HOSTED BY
ELSEVIER
Available online at www.sciencedirect.com
ScienceDirect
Soils and Foundations 58 (2018) 615–626
www.elsevier.com/locate/sandf

Hypoplastic model for crushable sand

N.T.V. Phuong [a,b,*], A. Rohe [b,d], R.B.J. Brinkgreve [a,c], A.F. van Tol [a,b]

[a] *Delft University of Technology, Delft, The Netherlands*
[b] *Deltares, Delft, The Netherlands*
[c] *Plaxis, Delft, The Netherlands*
[d] *University of Cambridge, Cambridge, UK*

Received 26 May 2016; received in revised form 29 January 2018; accepted 8 February 2018
Available online 6 July 2018

Abstract

A constitutive model for granular materials which considers grain crushing effects is developed in the framework of hypoplasticity. As grain crushing occurs the behaviour of granular material can usually be significantly affected. Several empirical relations between peak strength, uniformity coefficient and stiffness of sand depending on stress level or amount of grain crushing have been derived in the past. In this paper, such relations are employed to improve a basic hypoplastic constitutive model based on the changes of stress level or grain size distribution. In the proposed modified hypoplastic model only two additional physical parameters, namely uniformity coefficient and mean grain size are incorporated. The validation of the modified model for three different sands under triaxial test response with cell pressures up to 30 MPa is presented and shows a significantly better correspondence with regard to the original basic hypoplastic model.

Keywords: Hypoplastic model; Grain crushing

1. Introduction

Many researches in soil mechanics have focused on soil behaviour at low stress levels which is suitable for most geotechnical engineering problems. However, there are several geotechnical applications which need thorough investigation of high stress conditions, as e.g. high earth dams, deep mine shafts, tunnels, deep well shafts or deep jacked pile foundations. During penetration of a cone or pile in sand, the stress level around the pile tip can vary significantly from very low at rest (i.e. a few kPa) to very high soil stresses which may be up to 70 MPa (Murphy, 1987). As the effective confining stress around the pile increases, the strength of the surrounding soil (such as friction or dilatancy) may reduce. For sands, Bolton (1986) attributed this to the grain crushing strength. Yamamuro and Lade (1996) and Lade et al. (1996) studied the effects of grain crushing in drained and undrained triaxial compression and extension tests at confining stresses between 0.5 MPa and 52 MPa. They concluded that increases in confining stress cause a measured increase in the amount of grain crushing.

Hence, for applications involving large stress variations it is inevitable to have a stress dependent soil model which can be used across a wide stress range and accounts for crushing of soil grains. Daouadji et al. (2001) and Daouadji and Hicher (2010) introduced the influence of crushable grain in an elastoplastic model by making the critical state line dependent on the evolution of the grain size distribution. Comparing with experimental data for three different types of materials: a quartzic, calcareous sands and a rockfill material, the model simulations can accurately reproduce the stress-strain behaviour which demonstrates its ability to reproduce the main features of

Peer review under responsibility of The Japanese Geotechnical Society.
* Corresponding author at: Delft University of Technology, Delft, The Netherlands.
E-mail address: phuongnguyenviet137@gmail.com (N.T.V. Phuong).

https://doi.org/10.1016/j.sandf.2018.02.022
0038-0806/

sand behaviour subjected to grain crushing. However, the parameters controlling the amount of grain breakage along a given test have to be determined by curve fitting. Russell and Khalili (2004) presented a new bounding surface elastoplastic constitutive model for sands which is suited to a wide range of stress, including grain crushing. In this model, a unique shaped critical state line is defined to capture the three models of plastic deformation observed across a wide range of stresses, including particle rearrangement, particle crushing and pseudoelastic deformation. A good agreement between model simulations and experimental data from tests subject to five load paths was found. Furthermore, the basic concepts of critical state soil mechanics as well as a nonassociative flow rule commonly used in sand are confirmed to be valid when particle crushing occurs. Later, another bounding surface constitutive model based on Severn-Trent sand model was published, in which the critical state line was extended to include the effect of grain breakage through a grading state index (Fukumoto, 1992). The effect of crushing was found to shift the critical state line and compression line downwards in the compression plane. As a result, the state parameter tends to increase and the soil feels looser. In 2014, Engin et al. (2014) proposed a model which incorporates the effects of grain crushing at high stress levels, and which is a modification of Von Wolffersdorffs hypoplastic model. In this model, the void ratio is modified to be dependent on the uniformity coefficient, which is changing with vertical stress level. Their proposed model can model the suppressed dilatancy at high confinement stress level better than the original model, however, the simulation results are not so close with experimental ones. In addition, the performance of the model on the other hand has shown convergence issues during finite element simulations of boundary value problems.

In the first part of the paper, the relations between peak strength, uniformity coefficient and stiffness of sand depending on stress level and amount of grain crushing derived for different sands based on experimental results in literature are described. Then, a method to modify and improve a basic hypoplastic model in order to describe the behaviour of sand over a wide stress range, especially very high stress levels including grain crushing is developed. For the proposed modified hypoplastic model only two additional well-known physical parameters, namely the uniformity coefficient and the mean grain size are included. Those parameters are straightforward to determine, which is significantly simpler than currently existing models accounting for grain crushing (Hu et al., 2011; Engin et al., 2014).

The proposed modified hypoplastic model is validated using literature data of several triaxial test series for three different sands: Hostun sand in a stress range between 0.1 and 15 MPa (Colliat-Dangus et al., 1988), Toyoura sand in a stress range between 0.1 and 29.4 MPa (Miura and Yamanouchi, 1973) and Fontainebleau sand in a stress range between 0.1 and 30 MPa (Luong and Touati, 1983).

2. Behaviour of sand at high stress levels

2.1. Grain size and uniformity

2.1.1. Literature review

Grain size effects play a role in crushing strength, especially in brittle sand grain and rock aggregate. For a given shearing condition, the coarser the granular material is, the higher the grain breakage ratio (Marachi et al., 1969; Lee, 1992; Ovalle et al., 2014). Ovalle et al. (2014) also observed a slight decrease in the shear strength envelope for the coarser material. For instance, the maximum friction angle decreases about 2–3° for a particle size reduction factor of 4.

Fukumoto (1992) conducted one-dimensional compression tests on initially uniformly graded Ottawa sand to determine the grain size distribution at different applied vertical stresses between 7 MPa and 100 MPa. It was observed that with increasing effective vertical stress, the uniformity coefficient increases significantly. Nakata et al. (2001a,b) performed high-pressure one-dimensional compression tests on Silica sand samples, both initially uniformly graded and well-graded. They concluded that even for the same material the yielding characteristics depend on the initial grading curve with much more yielding occurring for uniformly graded sands in comparison to well-graded sands. As the material was changing from uniform to well-graded, the nature of grain crushing was changing from catastrophic onset to gradual breakage and rounding off surfaces.

It is observed that the change of the material characteristics can be captured by a change of the shape of the grain size distribution curve, characterized by the uniformity coefficient C_u (Biarez et al., 1994; Nakata et al., 2001b,a; Coop et al., 2004). Moreover the change of uniformity coefficient has a limit value and can be related to a change of applied effective stress. By using the test results of Nakata et al. (2001a), Rohe (2010) elaborated quantitatively the dependency of the uniformity coefficient on the applied (vertical) stress level characterized by the two stress invariants, namely mean effective stress p' (negative in compression) and deviatoric stress q and generalized as,

$$C_u = \alpha_p p'^2 - \alpha_q q^2 + \beta_p p' - \beta_q q + C_{u0} \quad (1)$$

in which α_p and α_q are the factors controlling the quadratic change of uniformity coefficient due to isotropic and deviatoric loading, respectively; β_p and β_q are the factors controlling the linear change of uniformity coefficient due to isotropic and deviatoric loading, respectively and C_{u0} is the reference uniformity coefficient at reference stress σ_{ref}. However, the determination of such factors was not elaborated and the suggested values are valid for a silica sand under one-dimensional compression only.

2.1.2. Generalize the dependency of the uniformity coefficient C_u on stress level

In order to generalize the dependency of the uniformity coefficient C_u on stress level under both triaxial and

one-dimensional compression response, the amount of grain crushing for different types of sands is derived with data collected from literature. An overview of investigated sands listing their reference uniformity coefficient C_{u0}, reference grain size diameter $d_{50,0}$, type of test and range of stress level during test is summarized in Table 1. Based on the test data the uniformity coefficient C_u is determined for different applied stress levels and illustrated in Fig. 1. The horizontal axis represents a non-dimensional stress which is the applied stress (vertical effective stress for oedometer test and cell pressure for triaxial test) multiplied by the reference uniformity coefficient C_{u0} and reference mean grain size $d_{50,0}$ in order to account for the influence of initial grain size distribution. σ_{ref} is the reference stress level of 100 kPa. d_{ref} is the reference grain diameter of 1 mm. The vertical axis represents the difference between current uniformity coefficient C_u and reference uniformity coefficient C_{u0} for increasing stress level.

From Fig. 1 it can be seen that triaxial tests (red markers) result in a higher amount of grain crushing than would occur for oedometer tests (blue markers) which can be attributed to the additional effects of shearing. Most of the sands in triaxial test conditions show a comparable amount of grain crushing, except Toyoura (6) and Sacramento river sand (7). These two sands result in a significant higher amount of crushing. This may be caused by the fact that only the samples of Toyoura and Sacramento river sand had enough time to achieve maximum densification after applying cell pressure, whereas in the other triaxial tests this issue was not considered (Miura and Yamanouchi (1973) found that the porosity of a sand at high pressure was affected not only by the magnitude of

Table 1
Overview of investigated sands.

N_0	Material	C_{u0}	$d_{50,0}$ [mm]	Test type	Stress level [MPa]	p^{ref} [kPa]	E^{ref} [kPa]	Reference
(1)	Fontainebleau sand	1.5	0.174	triaxial test	0.1–30	100	57,000	Luong and Touati (1983)
(2)	Hostun sand	1.69	0.32	triaxial test	0.1–15	50	22,727	Colliat-Dangus et al. (1988)
(3)	Cambria sand	1.3	1.6	triaxial test	2.1–60	100	53,700	Lade et al. (1996)
(4)	Chattahoochee river sand	2.47	0.37	triaxial test	0.1–62	98	30,000	Vesic and Clough (1968)
(5)	Quartz sand	1.83	0.31	triaxial test	0.1–7.8	115	30,000	Russell and Khalili (2004)
(6)	Toyoura sand	1.5	0.23	triaxial test	0.1–49	98	28,023	Miura and Yamanouchi (1973)
(7)	Sacramento river sand	1.57	0.2	triaxial test	0.1–13.7	98	34,000	Lee and Seed (1967)
(8)	Silica sand	2.17	0.75	oedometer test	0.1–92			Nakata et al. (2001b)
(9)	Ottawa sand	1.43	0.63	oedometer test	0.1–96.6			Fukumoto (1992)
(10)	Mono quartz sand 1	2	0.36	oedometer test	0.1–50			Chuhan et al. (2002)
(11)	Mono quartz sand 2	2.36	0.3	oedometer test	0.1–50			Chuhan et al. (2002)
(12)	Mono quartz sand 3	2.23	0.63	oedometer test	0.1–50			Chuhan et al. (2002)
(13)	Chattahoochee river sand	2.47	0.37	isotropic compression	0.1–62			Vesic and Clough (1968)
(14)	Hostun sand	1.69	0.32	oedometer test	0.1–100			Colliat-Dangus JL (1986)
(15)	Quartz sand	1.83	0.31	oedometer test	0.1–1000			Yamamuro et al. (1996)
(16)	Toyoura sand	1.5	0.23	isotropic compression	0.1–49			Miura and Yamanouchi (1973)

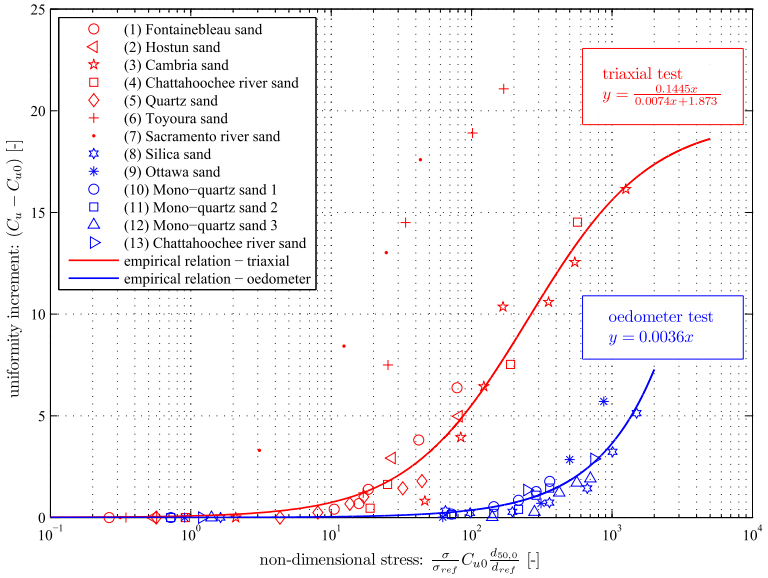

Fig. 1. Dependency of the uniformity coefficient on the stress level in triaxial compression tests (red) and in one–dimensional compression tests (blue) for various sands listed in Table 1.

the compression pressure but also by its duration. The influence of time on the compressibility of the sand is considerably large when the applied pressure is higher than 29 MPa. Maximum densification could not be reached before 350 or 570 h for a dense specimen compressed isotropically at a pressure of 30 or 50 MPa). On the other hand, the higher the degree of compression the greater part of grain crushing has been attained (Miura and Yamanouchi, 1973). Hence, at the same stress level, for samples of Toyoura and Sacramento river sand such higher values of uniformity coefficient are obtained compared to samples of other sands. For that reason, these two tests on Toyoura and Sacramento river sand are excluded for further study.

According to Fig. 1, an empirical relation for the dependency of C_u on stress level is suggested as following

- For triaxial response:

$$C_u = \frac{0.1445x}{0.0074x + 1.873} + C_{u0} \tag{2}$$

with

$$x = \frac{\sigma_{tx}}{\sigma_{ref}} C_{u0} \frac{d_{50,0}}{d_{ref}} \tag{3}$$

in which σ_{tx} is the cell pressure of a triaxial test, the reference pressure σ_{ref} is 100 kPa and the reference grain diameter d_{ref} is 1 mm.

- For oedometer response:

$$C_u = 0.0036x + C_{u0} \tag{4}$$

with

$$x = \frac{\sigma_{oed}}{\sigma_{ref}} C_{u0} \frac{d_{50,0}}{d_{ref}} \tag{5}$$

where σ_{oed} is the applied effective vertical stress of an oedometer test.

As the considered sands are mainly Quartz sands, the proposed relation may not be applicable for other types of sand which are more sensitive for crushing such as carbonate sediments, decomposed granite or residual soils. In addition, the effects of particle shape, particle size, initial grading, water content could cause some scatter when different sands are considered.

2.2. Minimum and maximum void ratio

2.2.1. Literature review

The maximum void ratio, e_{max}, is the void ratio corresponding to the loosest state of the grain assembly, the minimum void ratio, e_{min}, is the void ratio corresponding to its densest state. Some general properties following from Youd (1973), Cho et al. (2006), Biarez et al. (1994) are

- e_{min} decreases with increasing C_u due to filling of the voids between larger grains by smaller ones. e_{min} decreases with diminishing angularity of grains. e_{min} increases as roundness and sphericity decrease.
- e_{max} decreases with increasing C_u. e_{max} increases as particle roundness and particle sphericity decrease.

Rohe (2010) suggested that the change of maximum and minimum void ratio can be related to a change of the uniformity coefficient C_u and the shape of grains as

$$e_{min,max} = f(C_u(R,S)) \tag{6}$$

in which R is grain roundness and S is the grain sphericity. However, it is not straightforward to generalise Eq. (6) for various sands since information on R and S is often missing and complex to determine.

2.2.2. Elaborating empirical correlation between the void ratios and stress level

For the purpose of simplicity, an empirical correlation between the void ratios and stress level is elaborated replacing Eq. (6). During one dimensional tests, relations between σ_{oed} and the current void ratio are determined for both loosest and densest state of each sand. The loosest state of sand ($e_{loose\ considered}$) is used as reference for e_{max} and the densest state of sand ($e_{dense\ considered}$) is used as reference for e_{min}. Table 2 shows the value of void ratio used to build up the relation for e_{min} and e_{max}.

The decrease of minimum and maximum void ratio in oedometer tests for four different sands in Table 1 is quantified and illustrated in Fig. 2. The horizontal axis represents a non-dimensional stress which is the ratio between applied vertical effective stress of a oedometer test σ_{oed} and reference pressure σ_{ref} of 100 kPa. The vertical axis represents the change of minimum and maximum void ratio for increasing stress level: $\Delta e_{min} = e_{min} - e_{min,0}$ and $\Delta e_{max} = e_{max} - e_{max,0}$.

From Fig. 2 it can be seen that most of the sands show similar behaviour for stresses ranging between 0 and 100 MPa. Based on that, the following empirical relations are suggested for the change of minimum and maximum void ratio depending on stress level,

$$\Delta e_{min} = \frac{0.0132 \frac{\sigma_{oed}}{\sigma_{ref}}}{0.0159 \frac{\sigma_{oed}}{\sigma_{ref}} + 7.77} \tag{7}$$

$$\Delta e_{max} = \frac{0.0072 \frac{\sigma_{oed}}{\sigma_{ref}}}{0.0119 \frac{\sigma_{oed}}{\sigma_{ref}} + 6.37} \tag{8}$$

Table 2
Considered void ratios use to represent the minimum and maximum void ratio.

Sand	e_{min}	e_{max}	$e_{dense\ considered}$	$e_{loose\ considered}$
Hostun sand	0.61	0.96	0.67	0.9
Quartz sand			0.68	0.9
Toyoura sand	0.61	0.98	0.60–0.62	0.82–0.84
Silica sand	0.63	0.88	0.60–0.63	0.75

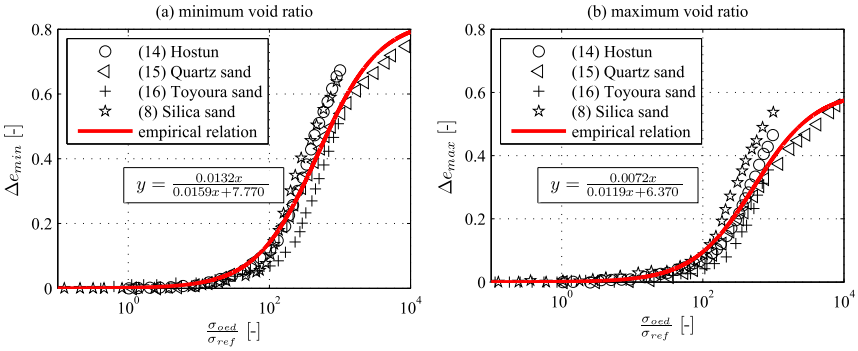

Fig. 2. Dependency of the minimum (a) and maximum (b) void ratio on stress level for various sands listed in Table 1.

These two relations are supposed to be applicable for Quartz sands and restricted for one dimensional loading mode only. The relations between maximum and minimum void ratio and triaxial loading mode are important and should be included in Eqs. (7) and (8). However the data needed to build up such relations is missing, which can be considered in future research.

2.3. Peak strength

Various investigations examining soil behaviour in triaxial compression tests at high confining stresses have been carried out in the past. In several conclusions regarding the Mohr-Coulomb secant friction angle at high stresses it is stated that the friction angle in compression decreases with increasing confining stress while approaching an asymptotical limit value at high stress (Vesic and Clough, 1968; Miura and Yamanouchi, 1973). Other researchers have found that the friction angle in compression tests decreases to a minimum value and then increases to a constant value at higher stress level (Lee and Seed, 1967; Colliat-Dangus et al., 1988; Yamamuro and Lade, 1996). It is also found that the volumetric and axial strains at failure in compression tests become more contractive with increasing confining stress (Lee and Seed, 1967; Vesic and Clough, 1968; Miura and Yamanouchi, 1973; Luong and Touati, 1983; Colliat-Dangus et al., 1988; Yamamuro and Lade, 1996).

Bolton (1986) proposed an empirical relation to express that the peak friction angle and dilatancy angle of a sand depend on the stress level. It yields

$$\varphi'_{max} - \varphi'_{crit} = 3I_R \tag{9}$$

The maximum dilatancy rate at failure state is defined as,

$$\left(\frac{-\mathrm{d}\varepsilon_{vol}}{\mathrm{d}\varepsilon_{vert}}\right)_{max} = 0.3I_R \tag{10}$$

φ'_{max} and φ'_{crit} are the maximum and critical state friction angle respectively, and the relative dilatancy index I_R (non-dimensional value) is defined as,

$$I_R = R_D[Q - \ln(p')] - R \tag{11}$$

in which R_D is the relative density of sand and p' is the applied mean effective stress level. Q and R are relative dilatancy indices for which Bolton suggested the values $Q = 10$ and $R = 1$ for Quartz sand. (The value of Q depends on the units taken for p': kPa is used here)

The dilatancy angle can be calculated from drained triaxial tests according to Schanz and Vermeer (1996) as follows,

$$\sin\psi = -\frac{\frac{\mathrm{d}\varepsilon_{vol}}{\mathrm{d}\varepsilon_{vert}}}{2 - \frac{\mathrm{d}\varepsilon_{vol}}{\mathrm{d}\varepsilon_{vert}}} \tag{12}$$

Combining Eqs. (10) and (12), the maximum dilatancy angle can be expressed in the form,

$$\sin\psi = \frac{0.3I_R}{2 + 0.3I_R} \tag{13}$$

The triaxial test results of Luong and Touati (1983) performed on very dense Fontainebleau sand ($e = 0.56, R_D = 95\%$) with different cell pressure levels ranging between 0.5 MPa and 30 MPa are used to evaluate above relationship. Results show that friction angle and dilatancy angle depend on mean stress level and can be calculated based on Bolton's relation (11), (9) and (13). The comparison between results of laboratory triaxial tests and the empirical relation is shown in Fig. 3. Based on the results it can be concluded that the relations derived by Bolton (1986) and Schanz and Vermeer (1996) are in

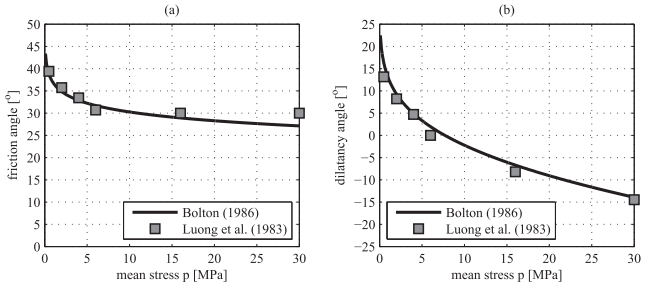

Fig. 3. Comparison of triaxial test data on Quartz sand ($R_D = 95\%$) at high stress levels (Bolton, 1986; Luong and Touati, 1983). (a) Relation between stress level and friction angle, (b) relation between stress level and dilatancy angle.

good agreement with the triaxial test results and can be used to describe the evolution of strength at high stress levels.

2.4. Stress dependency of stiffness

2.4.1. Literature review

Ohde (1939) studied the behaviour of sand in compression tests and derived the stress-dependent oedometer modulus following a power law as

$$E = E^{ref}\left(\frac{p}{p^{ref}}\right)^{w} \tag{14}$$

in which E^{ref} is the reference value of stiffness E_{50} at reference pressure p^{ref} (Table 1) and w is an exponential factor. Schanz and Vermeer (1998) concluded that for oedometer and triaxial tests the exponent w is in a range between 0.4 and 0.75 for different types of sands and influenced by the mean grain size d_{50} and the uniformity coefficient C_u. Jänke (1968) showed that w decreases with decreasing C_u, increasing angularity and increasing d_{50}. According to Herle and Gudehus (1999), the value of $w = 0.33$ is considered as a lower bound, corresponding to the behaviour of elastic spheres without rearrangements. $w = 1$ is the upper bound which represents the familiar straight compression line in a semi-logarithmic plot.

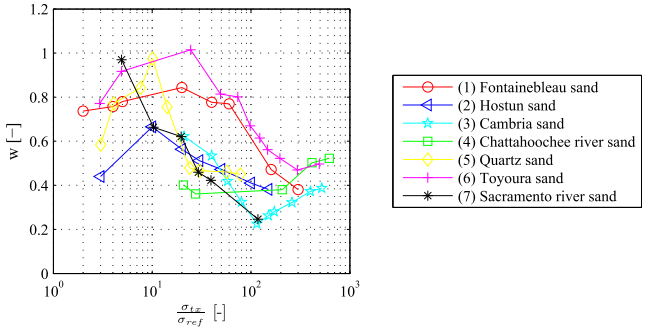

Fig. 4. Dependency of exponent w (Eq. (14)) on cell pressure level for various granular soils under triaxial test conditions for sands listed in Table 1.

2.4.2. Normalised function of stiffness depending on the stress level and grain crushing

To understand the dependency of exponent w on stress level, the value of w is calculated following Eq. (14), using data from triaxial test results for various sands. The results are illustrated in Fig. 4. It can be seen that the exponent w is in the range between 0.2 and 1. It is observed that during the increase of confining stress, the exponent w reaches its highest value, after which it reduces significantly towards a minimum and then it may rise somewhat.

Fig. 5 shows the dependency of w on both stress level and uniformity. The graph can be divided into three zones.

- Zone 1, $\left(\frac{\sigma_{1x}}{\sigma_{ref}} \cdot C_{u0} \cdot C_u \cdot \frac{d_{50,0}}{d_{ref}}\right) \leqslant 5 : w$ increases due to the densification of soil during loading. Assuming $w = 0.2$ is the lowest value for pressures from 0 to 200 kPa, the increase of w in zone 1 can be estimated as

$$w = (0.179\ln(x) + 0.712)R_D \tag{15}$$

where $x = \frac{\sigma_{1x}}{\sigma_{ref}} \cdot C_{u0} \cdot C_u \cdot \frac{d_{50,0}}{d_{ref}}$ and R_D is the relative density of sand

- Zone 2, $5 < \left(\frac{\sigma_{1x}}{\sigma_{ref}} \cdot C_{u0} \cdot C_u \cdot \frac{d_{50,0}}{d_{ref}}\right) \leqslant 1300 : w$ reduces significantly. In this zone, the soil starts to be crushed leading to a rapidly increasing C_u. The more crushing, the lower value of exponent w is obtained. w can be defined in zone 2 as

$$w = (0.126\ln(x) + 1.202)R_D \tag{16}$$

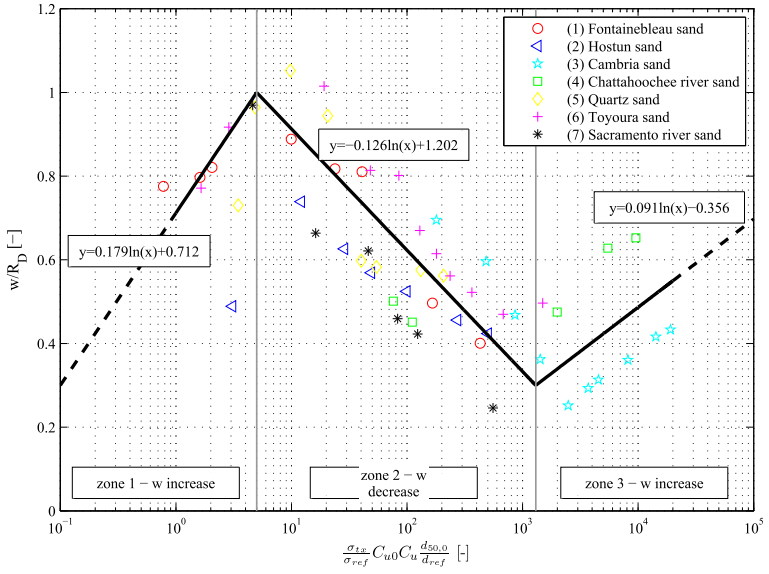

Fig. 5. Normalised function of w depending on pressure and uniformity.

- Zone 3, $\left(\frac{\sigma_{tr}}{\sigma_{ref}} \cdot C_{u0} \cdot C_u \cdot \frac{d_{50,0}}{d_{ref}}\right) > 1300$: crushing process is nearly finished, and soil is densifying again, hence a gradual increase of w is observed, which can be defined as

$$w = (0.091 \ln(x) - 0.356) R_D \tag{17}$$

The empirical relations in Eqs. (15)–(17) are used to estimate the value of w for increasing stress level and grain crushing for different sands. Hence, the dependency of stiffness on stress level can be calculated following Eq. (14).

It could be argued that if the data are not enough for a huge scatter in Fig. 5, then the empirical evidence is limited, but with the used expression for the parameters of influence, there seems to be a trend that indicates three stages in the evolution of the level of stress-dependency of stiffness, which is explained physically. A third order polynomial function could have been used, but instead the authors simply divided the function into three zones, and quantified the function constants based on the limited data. These constants, that are hard-coded in the model, could be updated in the future when more data is taken into consideration. The purpose here is to identify this trend in stress-level dependency and to describe it at least qualitatively.

To conclude, the empirical relations above are developed to estimate the dependency of the uniformity coefficient, void ratio, strength and stiffness on the stress level. In the following section, the implementation of such relations into a constitutive relationship is introduced.

3. Modified hypoplastic model for sand at high stress levels

Hypoplasticity is an anelastic (dissipative) and incrementally nonlinear constitutive theory of granular materials, which requires neither a yield surface nor a decomposition of strain rate into elastic and plastic portion (Niemunis, 2003). In the framework of hypoplastic constitutive relations dilation, contraction and the dependency of stiffness on stress and density is incorporated. The hypoplastic model was first proposed in 1978 by Kolymbas (1978). It suffered from difficulties in determining the input parameters as well as its physical meaning for such rate type constitutive equation. Until 1991, a solution was proposed by Kolymbas (1991) which combined the influences of pressure and density into the model. Later in 1996, the pressure-dependent limit void and stress ratios were introduced by Bauer (1996) and Gudehus (1996) into the hypoplastic relation. This lead to a possible easy and robust way of model parameter determination and consequently, more and more validation of the model with laboratory tests. A shortcoming of the model by Bauer and Gudehus was that it did not predict proper shape of the critical state locus in the octahedral plane. Hence, another modification of the model is attributed to von Wolffersdorff (1996), who modified the Lode-angle dependency in such a way that it corresponds to the Matsuoka-Nakai limit surface.

The hypoplastic constitutive model by von Wolffersdorff (1996) will be used in this study as the basic model for further development. The Cauchy (effective) stress tensor $\boldsymbol{\sigma}$ and the void ratio e are state variables. It is assumed that the soil is a homogeneous granular body whose state is fully described by these two state variables. The constitutive relation is presented in the form which consists of terms linear in strain rate similar to hypoelasticity as well as additional terms that are nonlinear in strain rate. It is written as

$$\overset{\circ}{\boldsymbol{\sigma}} = f_s(\mathbf{L} : \dot{\boldsymbol{\varepsilon}} + f_d \mathbf{N} \|\dot{\boldsymbol{\varepsilon}}\|) \tag{18}$$

$$\mathbf{L} = F^2 \dot{\boldsymbol{\varepsilon}} + a^2 \mathrm{tr}(\hat{\boldsymbol{\sigma}} \cdot \dot{\boldsymbol{\varepsilon}}) \hat{\boldsymbol{\sigma}} \tag{19}$$

$$\mathbf{N} = aF \|\dot{\boldsymbol{\varepsilon}}\| (\hat{\boldsymbol{\sigma}} + \hat{\boldsymbol{\sigma}}_d) \tag{20}$$

it yields

$$\overset{\circ}{\boldsymbol{\sigma}} = f_e f_b \frac{1}{\mathrm{tr}(\hat{\boldsymbol{\sigma}}^2)} \left[F^2 \dot{\boldsymbol{\varepsilon}} + a^2 \mathrm{tr}(\hat{\boldsymbol{\sigma}} \cdot \dot{\boldsymbol{\varepsilon}}) \hat{\boldsymbol{\sigma}} + f_d aF \|\dot{\boldsymbol{\varepsilon}}\| (\hat{\boldsymbol{\sigma}} + \hat{\boldsymbol{\sigma}}_d)\right] \tag{21}$$

in which $\mathbf{L}$ and $\mathbf{N}$ are the fourth and second order constitutive tensors, respectively, both functions of stress. The first part in Eq. (18) is the hypoelastic part which linear in $\dot{\varepsilon}$ and the second part is non-linear in $\dot{\varepsilon}$ due to the Euclidean norm of the strain rate tensor $\|\dot{\varepsilon}\| = \sqrt{\mathrm{tr}^2(\dot{\varepsilon})}$.

Further,

$$\hat{\boldsymbol{\sigma}} = \frac{\boldsymbol{\sigma}}{\mathrm{tr}(\boldsymbol{\sigma})} \tag{22}$$

is the stress ratio tensor and

$$\hat{\boldsymbol{\sigma}}_d = \hat{\boldsymbol{\sigma}} - 1/3\mathbf{I} \tag{23}$$

is the deviatoric part of $\hat{\boldsymbol{\sigma}}$ and $\mathbf{I}$ is the unit tensor.

The scalars a and F, in Eq. (21) depend on the invariants of the Cauchy stress tensor $\boldsymbol{\sigma}$ and the void ratio e. They determine the Matsuoka-Nakai critical state surface in stress space as

$$a = \frac{\sqrt{3}(3 - \sin\varphi_c)}{2\sqrt{2}\sin\varphi_c} \tag{24}$$

in which φ_c is the friction angle in critical states and

$$F = \sqrt{\frac{1}{8}\tan^2\psi + \frac{2 - \tan^2\psi}{2 + \sqrt{2}\tan\psi\cos 3\vartheta}} - \frac{1}{2\sqrt{2}}\tan\psi \tag{25}$$

in which the invariants $\tan\psi$ and $\cos 3\vartheta$ read

$$\tan\psi = \sqrt{3}\|\hat{\boldsymbol{\sigma}}_d\| \tag{26}$$

and

$$\cos 3\vartheta = -\sqrt{6}\frac{\mathrm{tr}(\hat{\boldsymbol{\sigma}}_d^3)}{[\mathrm{tr}(\hat{\boldsymbol{\sigma}}_d^2)]^{\frac{3}{2}}} \tag{27}$$

The scalar F specifies the shape of the Matsuoka-Nakai yield function. The critical state surface of this model can be written as

$$f = \frac{1}{2}\|\hat{\boldsymbol{\sigma}}\| - F^2 \frac{4\sin\varphi_c}{3(3-\sin\varphi_c)} \tag{28}$$

The pycnotropic functions f_d and f_e in Eq. (21) are density dependent which are defined as

$$f_d = \left(\frac{e-e_d}{e_c-e_d}\right)^{\alpha}, \qquad f_e = \left(\frac{e_c}{e}\right)^{\beta} \tag{29}$$

and the barotropic function f_b is pressure dependent which is written as

$$f_b = \frac{h_s}{n}\left(\frac{1+e_i}{e_i}\right)\left(\frac{e_{i0}}{e_{c0}}\right)^{\beta}\left(-\frac{\mathrm{tr}(\boldsymbol{\sigma})}{h_s}\right)^{1-n}\left[3+a^2-\sqrt{3}a\left(\frac{e_{i0}-e_{d0}}{e_{c0}-e_{d0}}\right)^{\alpha}\right]^{-1} \tag{30}$$

in which α, β, n are material factors which are constant in the exponents; h_s is the granular hardness; e_{c0}, e_{d0}, e_{i0} are the critical void ratio, the minimum void ratio and the maximum void ratio at zero mean pressure, respectively. Altogether, there are eight parameters defining the basic hypoplastic model according to von Wolffersdorff (1996), i.e. $\varphi_c, h_s, n, e_{d0}, e_{c0}, e_{i0}, \alpha$ and β.

Such parameters are usually calibrated at low stress levels ($0-200$ kPa) for which they are assumed to be constant. As shown in Section 2, high stress levels and grain crushing may have a significant influence on the material behaviour. In the following section a method will be introduced to modify the hypoplastic model such that high stress levels and grain crushing behaviour can be considered.

3.1. Modified minimum and maximum void ratio

Based on a regression analysis of experimental data of oedometer tests, Section 2.2 shows the dependency of the reference void ratio on the applied vertical stress. As a consequence of grain crushing, both minimum and maximum void ratios decrease with the increasing applied stress (see Fig. 2). Therefore it is proposed to redefine reference void ratios at each stress level to account for grain crushing. Based on the initial values of reference void ratios at zero pressure, e_{d0} and e_{c0}, the generalized form of modified reference void ratios according to Rohe (2010) and Engin et al. (2014) can be defined as

$$e^m_{d0} = e_{d0} - \Delta e_{min} \tag{31}$$

$$e^m_{c0} = e_{c0} - \Delta e_{max} \tag{32}$$

and

$$e^m_{i0} = 1.15 e^m_{c0} \tag{33}$$

where Δe_{min} and Δe_{max} follow the correlations in Eq. (7) and (8), respectively. The effects of modifying reference void ratios depending on stress levels are shown in Fig. 6.

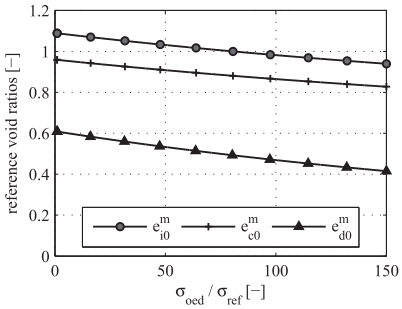

Fig. 6. Dependency of reference void ratios on stress level (for Hostun sand, $R_D = 90\%$).

3.2. Modified parameter α

Herle and Gudehus (1999) indicated that the peak state in a triaxial compression test simulation with the hypoplastic model can be controlled by considering the exponent α. They defined the following relation between α and maximum friction angle

$$\alpha = \frac{\ln\left[6\frac{(2+K_p)^2+a^2K_p(K_p-1-\tan\nu_p)}{a(2+K_p)(5K_p-2)\sqrt{4+2(1+\tan\nu_p)^2}}\right]}{\ln((e-e_d)/(e_c-e_d))} \tag{34}$$

With the peak ratios

$$K_p = \frac{1+\sin\varphi_p}{1-\sin\varphi_p} \tag{35}$$

$$\tan\nu_p = 2\frac{K_p-4+5AK_p^2-2AK_p}{(5K_p-2)(1+2A)} - 1 \tag{36}$$

in which

$$A = \frac{a^2}{(2+K_p)^2}\left[1-\frac{K_p(4-K_p)}{5K_p-2}\right] \tag{37}$$

and

$$a = \frac{\sqrt{3}(3-\sin\varphi_c)}{2\sqrt{2}\sin\varphi_c} \tag{38}$$

The value of friction angle at peak φ_p is determined following Bolton's Eq. (9) which is stress dependent. Hence, it is possible to determine α corresponding to each stress level as shown in Fig. 7 for a reference stress of $\sigma_{ref} = 100$ kPa. The value of exponent α reduces significantly with increasing stress level, and can even become negative.

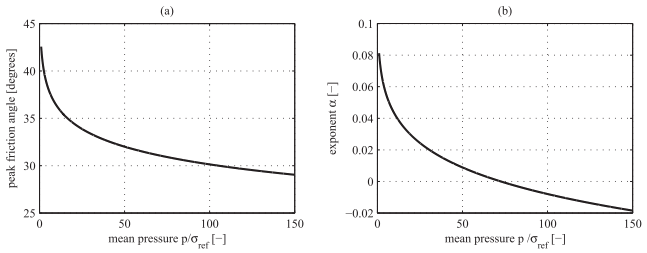

Fig. 7. Relation between (a) friction angle at peak φ_p versus mean pressure p and (b) exponent α versus mean pressure p (for Hostun sand, $R_D = 90\%$).

3.3. Modified parameter β

Through the factor $f_s = f_e \cdot f_b$ the calculated stiffness modulus E increases with increasing density and stress level (Herle and Gudehus, 1999). For a measured E corresponding to particular stress level, density and direction of stretching, exponent β can be calculated from Eq. (21), thus it follows

$$\beta = \frac{\ln\left[E\frac{3+a^2-f_{d0}a\sqrt{3}}{3+a^2-f_d a\sqrt{3}}\frac{e_i}{1+e_i}\frac{n}{h_s}\left(\frac{3p_s}{h_s}\right)^{n-1}\right]}{ln(e_i/e)} \tag{39}$$

Herle and Gudehus (1999) suggested to determine parameter β by considering the ratio of stiffness modulus at two different void ratios but at the same stress level. Hence, β is constant and the influence of p_s in the calculation of β is neglected. Using this approach, β is limited to the range of $0 \leqslant \beta \leqslant 2.5$ and $\beta \approx 1$ is obtained for many sands.

For the modified hypoplastic model exponent β is proposed to be defined alternatively. Consider a sand which has the same initial void ratio but at different stress level, Eq. (39) then becomes

$$\frac{\left(\frac{e_{i1}}{e_1}\right)^{\beta_1}}{\left(\frac{e_{i2}}{e_2}\right)^{\beta_2}} = \frac{E_1}{E_2}\frac{3+a^2-f_{d2}a\sqrt{3}}{3+a^2-f_{d1}a\sqrt{3}}\frac{e_{i1}}{1+e_{i1}}\frac{1+e_{i2}}{e_{i2}}\left(\frac{P_1}{P_2}\right)^{(n-1)} \tag{40}$$

in which the hypoplastic void ratios depend on the mean stress and are defined as

$$\frac{e_i}{e_{i0}} = \frac{e_c}{e_{c0}} = \frac{e_d}{e_{d0}} = \exp\left[-\left(\frac{-\mathrm{tr}\boldsymbol{\sigma}}{h_s}\right)^n\right] = \exp\left[-\left(\frac{-3p_s}{h_s}\right)^n\right] \tag{41}$$

Hence, $f_{d1} = f_{d2}$ and the term $\frac{3+a^2-f_{d2}a\sqrt{3}}{3+a^2-f_{d1}a\sqrt{3}}$ becomes 1.

The relation between stiffness E and mean stress p follows the power law in Eq. (14). Therefore, $E_1/E_2 = (P_1/P_2)^w$ and Eq. (40) can be written as

$$\left(\frac{e_{i2}}{e_2}\right)^{\beta_2} = \left(\frac{e_{i1}}{e_1}\right)^{\beta_1}\frac{1+e_{i1}}{e_{i1}}\frac{e_{i2}}{1+e_{i2}}\left(\frac{P_2}{P_1}\right)^{w+n-1} \tag{42}$$

Consider β_1 is the reference value of β which is determined following Herle and Gudehus (1999) at a reference mean stress p_1 of 100 kPa, hence

$$\beta_2 = \frac{\ln\left[\left(\frac{e_{i1}}{e_1}\right)^{\beta_{ref}}\frac{1+e_{i1}}{e_{i1}}\frac{e_{i2}}{1+e_{i2}}\left(\frac{P_2}{P_{ref}}\right)^{w+n-1}\right]}{ln\left(\frac{e_{i2}}{e_2}\right)} \tag{43}$$

where w is defined by Eqs. (15)–(17)

The relation between β and mean stress p is shown in Fig. 8 for Hostun sand. A slight increase in β at low stress level to a peak value of about 2.5 can be observed, after which a significant decrease of β from 2.5 to −2.5 follows.

In summary, a modified hypoplastic model is proposed in such way that parameters $e_{c0}, e_{d0}, e_{i0}, \alpha, \beta$ are stress dependent. For the basic hypoplastic model, there are eight parameters to be determined: $\varphi_c, h_s, n, e_{c0}, e_{d0}, e_{i0}, \alpha, \beta$. In the modified hypoplastic model, nine parameters need to be determined: $\varphi_c, h_s, n, e_{c0}, e_{d0}, e_{i0}, \beta_{ref}, C_{u0}$ and d_{50}. Parameter α can be eliminated as it is calculated directly from the mean stress level. β_{ref} is the value of β at reference stress level of 100 kPa. C_{u0} and d_{50} are two additional physical input parameters used to account for grain crushing. The determination of standard hypoplastic parameters follows Herle and Gudehus (1999).

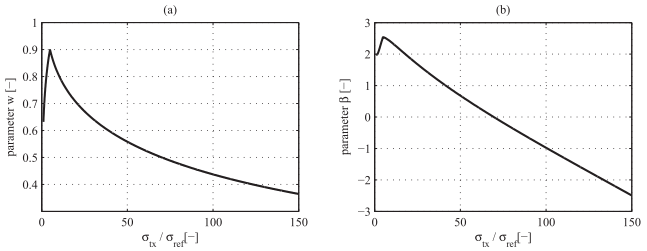

Fig. 8. Relation between exponent β versus normalised stress p (for Hostun sand, $R_D = 90\%$).

4. Validation of the modified hypoplastic model

The modified hypoplastic model is validated by simulating several triaxial tests for three different sands, i.e. Hostun, Fontainebleau and Toyoura at stress levels between 0.5 and 30 MPa. The modified hypoplastic model is implemented in UMAT format (Gudehus et al., 2008) and triaxial test simulations are done using a single Gauss point element test. The numerical results are compared with laboratory test results which are available in literature. The hypoplastic input parameters (which were calibrated for stress levels between 50 and 500 kPa) for the three sands are listed in Table 3.

In the previous section, it is suggested to modify the reference void ratios, exponent α and exponent β depending on the stress level. The effects of each parameter adaption are illustrated in Fig. 9 for Hostun dense sand with relative density of 90%. Note that the simulations are carried out with the original parameters of Table 2 which where determined for the reference stress level. At a cell pressure of 10 MPa, the original hypoplastic model predicts too high peak friction angle and too much dilatancy, whereas in the triaxial test, the friction angle tends towards the critical value and only contractive behaviour is observed. In other words, in the simulation the dense Hostun sand at very high cell pressure behaves in a quite similar way as loose sand. The modification for the reference void ratio suggested by Rohe (2010) and Engin et al. (2014) only slightly improves the peak strength and dilative behaviour. The modification of α results in quite accurate peak friction angle compared to the test, however, the soil stiffness is still too high. Finally, using also the modification of exponent β, the stiffness and dilative behaviour is reduced significantly to correspond with the test data. Hence, the modified hypoplastic model proposed in the previous section

Table 3
Hypoplastic parameters for Hostun sand (Herle and Gudehus, 1999), Toyoura sand (Herle and Gudehus, 1999) and Fontainebleau sand (Luong and Touati, 1983).

Parameter	φ_c [°]	h_s [MPa]	n	e_{d0}	e_{c0}	e_{i0}	α	β	C_{u0}	d_{50} [mm]
Hostun	32	1000	0.29	0.61	0.96	1.09	0.13	2.0	1.69	0.32
Toyoura	32	120	0.69	0.61	0.98	1.13	0.12	1.0	1.5	0.23
Fontainebleau	32	10000	0.56	0.54	0.94	1.08	0.08	1.2	1.48	0.174

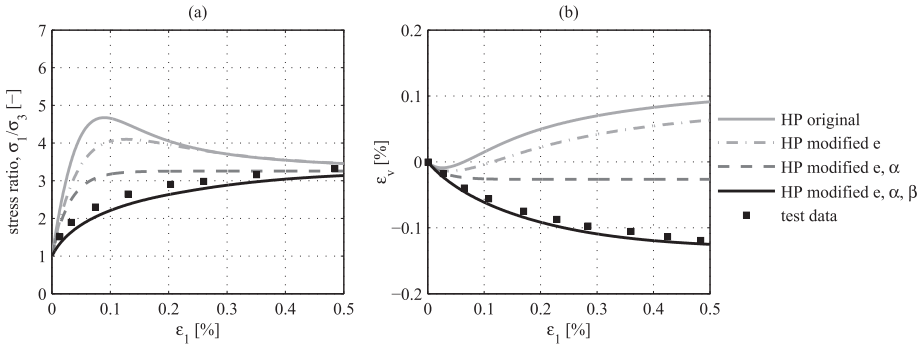

Fig. 9. Triaxial response of dense Hostun sand ($R_D = 90\%$) at high cell pressures of 10 MPa. Comparison of test result (Colliat-Dangus et al., 1988) with different hypoplastic model modifications. (a) Stress ratio versus vertical strain, (b) volumetric strain versus vertical strain.

results in simulations which are in good agreement with the triaxial laboratory test results.

More sands at different stress levels were selected to validate the model. Figs. 10–12 show the comparison between triaxial simulations at increased cell pressure using the original and the modified hypoplastic model with test results for three sands: Hostun sand, Toyoura sand and Fontainebleau sand, respectively. Each figure is divided into three rows, in which the first row shows the laboratory test results (Figure a and b), the second row shows the simulation results using the original hypoplastic model (Figure c and d) and the last one shows the simulation results using the modified hypoplastic model (Figure e and f). In the first column of each figure the relation between stress ratio σ_1/σ_3 and axial strain ε_1 is plotted, and the second column illustrates the relation of volumetric strain ε_v versus axial strain ε_1. For all simulations using the original hypoplastic model of all three sands, there is no contractive behaviour observed even at very high confining stresses (Figs. 10d, 11d and 12d). Moreover, the use of a constant value for α in the original hypoplastic model overestimates the peak friction angle, especially at high stress levels, whereas, the modified hypoplastic model results in quite accurate peak strength compared to the test data of all three sands. At

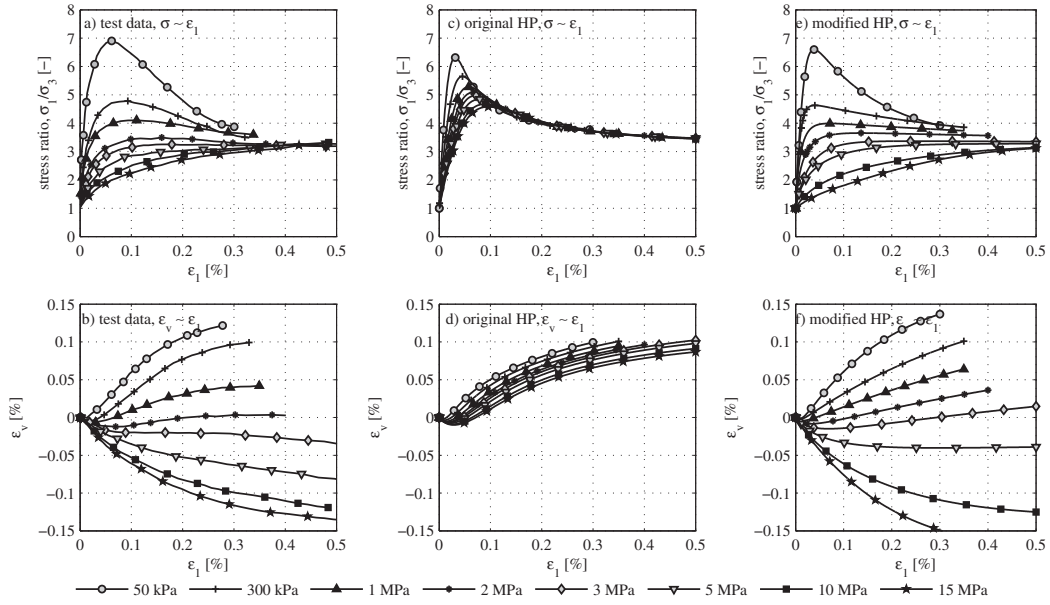

Fig. 10. Triaxial response of Hostun sand at cell pressures between 50 kPa and 15 MPa, (a) and (b) are test results (Colliat-Dangus et al., 1988), (c) and (d) are simulation results using original hypoplastic model, (e) and (f) are simulation results using modified hypoplastic model.

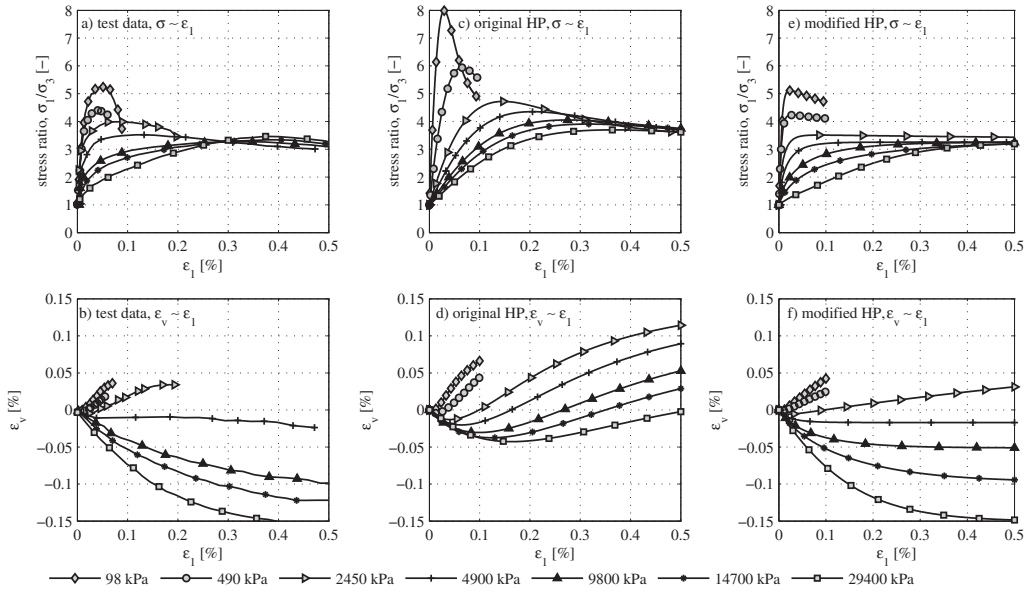

Fig. 11. Triaxial response of Toyoura sand at cell pressures between 98 kPa and 29400 kPa, (a) and (b) are test results (Miura and Yamanouchi, 1973), (c) and (d) are simulation results using original hypoplastic model, (e) and (f) are simulation results using modified hypoplastic model.

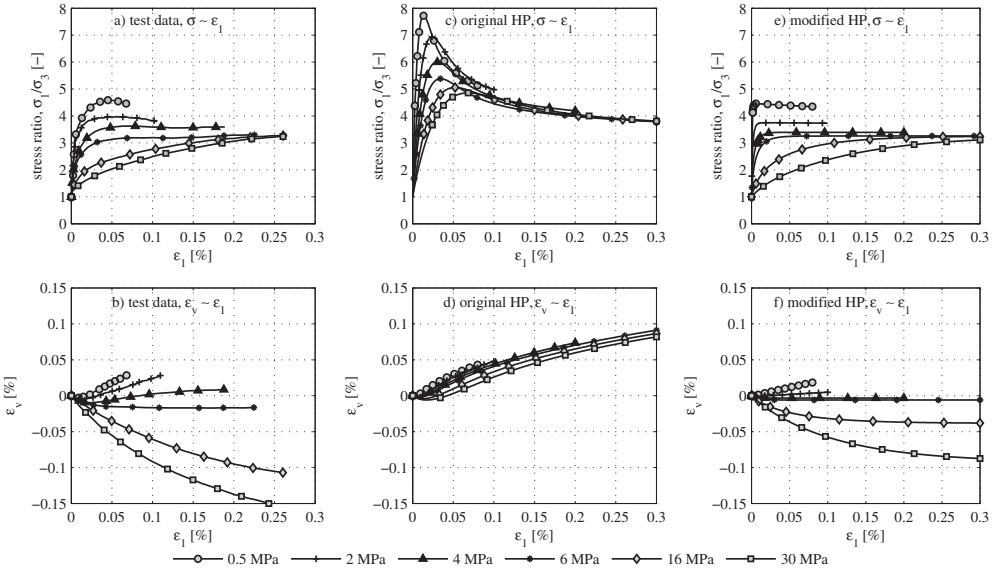

Fig. 12. Triaxial response of Fontainebleau sand at cell pressures between 500 kPa and 30 MPa, (a) and (b) are test results (Luong and Touati, 1983), (c) and (d) are simulation results using original hypoplastic model, (e) and (f) are simulation results using modified hypoplastic model.

very high stress level (larger than 5 MPa) the modified hypoplastic model results in a soil stiffness response that is much softer than for the original hypoplastic model which is quite similar to the test results. From the test data in Figs. 10a, 11a and 12a, it is observed that there is a slight reduction of critical state friction angle to lower values with increasing stress level. In the case of Toyoura sand, Fig. 11a, after reduction to a low value, the critical state friction angle rises somewhat. Hence, further studies are necessary to get a better understanding of the change of the critical state friction angle when crushing occurs.

To summarise, the validation of the modified hypoplastic model using triaxial test data shows the added value with regard to the original hypoplastic model. This indicates that the modified hypoplastic model considering grain crushing effects is very well suited to model the behaviour of sands for a wide range of stress levels.

5. Conclusion

The characteristics of sand at high stress levels and related to grain crushing are analysed. Based on these analyses, it is proposed to modify and improve the hypoplastic constitutive model to account for the influence of grain crushing. In the modified model, two well-known physical parameters, uniformity coefficient C_u and mean grain size diameter d_{50}, are included. Such parameters are straightforward to determine making the proposed model convenient

to use. Triaxial tests on three different sands were used to calibrate and validate the model. Comparison between experimental data and numerical simulations demonstrates that the modified hypoplastic model is capable of predicting both stress and strain accurately.

References

Bauer, E., 1996. Calibration of a comprehensive hypoplastic model for granular materials. Soils Found. 36 (1), 13–26.

Biarez, J., Hicher, P.Y., et al., 1994. Elementary Mechanics of Soil Behaviour: Saturated Remoulded Soils. Balkema, Rotterdam.

Bolton, M., 1986. The strength and dilatancy of sands. Geotechnique 36 (1), 65–78.

Cho, G.C., Dodds, J., Santamarina, J.C., 2006. Particle shape effects on packing density, stiffness, and strength: natural and crushed sands. J. Geotech. Geoenviron. Eng. 132 (5), 591–602.

Chuhan, F.A., Kjeldstad, A., Bjørlykke, K., Høeg, K., 2002. Porosity loss in sand by grain crushing, experimental evidence and relevance to reservoir quality. Mar. Pet. Geol. 19 (1), 39–53.

Colliat-Dangus, J,L., 1986. Comportement des matériaux Granulaires sous fortes contraintes (Ph.D. thesis). Université de Grenoble.

Colliat-Dangus, J.L., Desrues, J., Foray, P., 1988. Triaxial testing of granular soil under elevated cell pressure. In: Advanced Triaxial Testing of Soil and Rock, ASTM STP 977, pp. 290–310.

Coop, M., Sorensen, K., Freitas, T.B., Georgoutsos, G., 2004. Particle breakage during shearing of a carbonate sand. Géotechnique 54 (3), 157–164.

Daouadji, A., Hicher, P.Y., 2010. An enhanced constitutive model for crushable granular materials. Int. J. Numer. Anal. Methods Geomech. 34 (6), 555–580.

Daouadji, A., Hicher, P.Y., Rahma, A., 2001. An elastoplastic model for granular materials taking into account grain breakage. Eur. J. Mech. A/Solids 20 (1), 113–137.

Engin, H., Jostad, H., Rohe, A., 2014. On the modelling of grain crushing in hypoplasticity. In: International Conference on Numerical Methods in Geotechnical Engineering, NUMGE, Delft, The Netherlands.

Fukumoto, T., 1992. Particle breakage characteristics of granular soils. Soils Found. 32 (1), 26–40.

Gudehus, G., 1996. A comprehensive constitutive equation for granular materials. Soils Found. 36 (1), 1–12.

Gudehus, G., Amorosi, A., Gens, A., Herle, I., Kolymbas, D., Mašín, D., Muir Wood, D., Niemunis, A., Nova, R., Pastor, M., et al., 2008. The soilmodels. info project. Int. J. Numer. Anal. Meth. Geomech. 32 (12), 1571–1572.

Herle, I., Gudehus, G., 1999. Determination of parameters of a hypoplastic constitutive model from properties of grain assemblies. Mech. Cohes. Frict. Mater. 4 (5), 461–486.

Hu, W., Yin, Z., Dano, C., Hicher, P.Y., 2011. A constitutive model for granular materials considering grain breakage. Sci. China Technol. Sci. 54 (8), 2188–2196.

Jänke, S., 1968. Zusammendrückbarkeit und scherfestigkeit nichtbindiger erdstoffe: ihre quantitative ermittlung mit hilfe einfacher kennwerte und feststellung der sie bestimmenden einflussfaktoren. Baumaschine und Bautechnik, pp. 15.

Kolymbas, D., 1978. Ein nichtlineares viskoplatisches Stoffgesetz für Böden. Institut für Bodenmechanik und Felsmechanik, Universität Fridericiana in Karlsruhe.

Kolymbas, D., 1991. An outline of hypoplasticity. Arch. Appl. Mech. 61 (3), 143–151.

Lade, P.V., Yamamuro, J.A., Bopp, P.A., 1996. Significance of particle crushing in granular materials. J. Geotech. Eng. 122 (4), 309–316.

Lee, D.M., 1992. Angles of Friction of Granular Fills [Ph.D. thesis]. University of Cambridge.

Lee, K.L., Seed, H.B., 1967. Drained strength characteristics of sands. J. Soil Mech. Found. Div.

Luong, M., Touati, A., 1983. Sols grenus sous fortes contraintes. Rev. Fr. Géotech. (24), 51–63

Marachi, N., Chan, C., Seed, H., Duncan, J., 1969. Strength and deformation characteristics of rockfills materials. Technical Report TE-69-5. Department of Civil Engineering, University of California, Berkeley.

Miura, N., Yamanouchi, T., 1973. Compressibility and drained shear characteristics of a sand under high confining pressures. Technol. Rep. Yamaguchi Univ. 1 (2), 271–290.

Murphy, D.J., 1987. Stress, Degradation, and Shear Strength of Granular Material. Geotechnical Modeling and Applications. Gulf Publishing Company, Houston, pp. 181-211.

Nakata, Y., Hyodo, M., Hyde, A.F.L., Kato, Y., Murata, H., 2001a. Microscopic particle crushing of sand subjected to high pressure one-dimensional compression. Soils Found. 41 (1), 69–82.

Nakata, Y., Kato, Y., Hyodo, M., Hyde, A.F.L., Murata, H., 2001b. One-dimensional compression behaviour of unuformly granded sand related to single particle crushing strength. Soils Found. 41 (2), 39–51.

Niemunis, A., 2003. Extended Hypoplastic Models for Soils, vol. 34. Inst. für Grundbau und Bodenmechanik.

Ohde, J., 1939. Zur theorie der druckverteilung im baugrund.

Ovalle, C., Frossard, E., Dano, C., Hu, W., Maiolino, S., Hicher, P.Y., 2014. The effect of size on the strength of coarse rock aggregates and large rockfill samples through experimental data. Acta Mech. 225 (8), 2199.

Rohe, A., 2010. On the Modelling of Grain Crushing in Hypoplasticity. Technical Report. Delft University of Technology.

Russell, A.R., Khalili, N., 2004. A bounding surface plasticity model for sands exhibiting particle crushing. Can. Geotech. J. 41 (6), 1179–1192.

Schanz, T., Vermeer, P., 1996. Angles of friction and dilatancy of sand. Géotechnique 46 (1), 145–152.

Schanz, T., Vermeer, P., 1998. On the stiffness of sands. Géotechnique 48, 383–387.

Vesic, A.S., Clough, G.W., 1968. Behavior of granular materials under high stresses. J. Soil Mech. Found. Div.

von Wolffersdorff, P.A., 1996. A hypoplastic relation for granular materials with a predefined limit state surface. Mech. Cohes. Frict. Mater. 1 (3), 251–271.

Yamamuro, J.A., Bopp, P.A., Lade, P.V., 1996. One-dimensional compression of sands at high pressures. J. Geotech. Eng. 122 (2), 147–154.

Yamamuro, J.A., Lade, P.V., 1996. Drained sand behavior in axisymmetric tests at high pressures. J. Geotech. Eng. 122 (2), 109–119.

Youd, T., 1973. Factors controlling maximum and minimum densities of sands. In: Evaluation of Relative Denisty and its Role in Geotechnical Projects Involving Cohesionless Soils, vol. 523, pp. 98–112.